Electronic Supplementary Material (ESI) for Inorganic Chemistry Frontiers.

Supporting Information

Coupling of water-splitting mechanism and doping-mixture to design a novel Cr-perovskite for rapid and efficient solar thermochemical H_2 production

Jian Cong,[a,b] Tianzeng Ma,[a,b] Zheshao Chang,[a] ,Jasurjon S. Akhatov,[c] Mingkai Fu,[a,*] Xin Li [a, b, *]

[a] Institute of Electrical Engineering, Chinese Academy of Sciences, 100190, Beijing, China

[b] University of Chinese Academic of Sciences, 100049, Beijing, China

[c] Physical-Technical Institute, SPA "Physics-Sun", Tashkent, 100084, Uzbekistan

*Corresponding authors. E-mail addresses: fumingkai@mail.iee.ac.cn, drlixin@mail.iee.ac.cn

Experimental Section

The experimental setup of the thermochemical reaction is shown in the Fig. S1. In the redox process, the main equipment includes a tubular furnace with a corundum reaction chamber, a syringe pump to inject water, a steam generator to evaporate the injected water, and a gas chromatograph to analyze the concentration of H_2 and O_2. The experimental setting parameters of equipment are listed in the Table 1.

Table S1. Experimental details

Equipment	Setting Parameters
Tubular furnace (SK-G05163)	Heating rate: 10 °C/min, T = 0 ~1600 °C
Syringe pump	water injection velocity: 0~1 ml min^{-1}
Steam generator (FD-HG)	Evaporation temperature: 100 ~ 150 °C
Gas chromatograph (GC-2014C)	Tracer gas: H_2, O_2

There are three parts of experimental system. The first part is the gas pipeline, with heat tracing device (130 °C), to deliver the inert gas (argon) and water vapor into the reaction chamber. The carriers of analyzing O_2 and H_2 is Argon gas. In the reduction process, argon with the rate of 200 ml min^{-1} flows into reaction chamber to provide an inert environment, and in the oxidation process, the mixing gas (vapor-argon) flows into the chamber to react with the sample powder hold in a corundum crucible. The water injection rate is controlled at 0.5 ml min^{-1}. This part of the system is the reaction region. After the redox reaction, the produced gas flows through a gas-liquid separator to remove water vapor and then the produced H_2 is analyzed by the gas chromatograph.

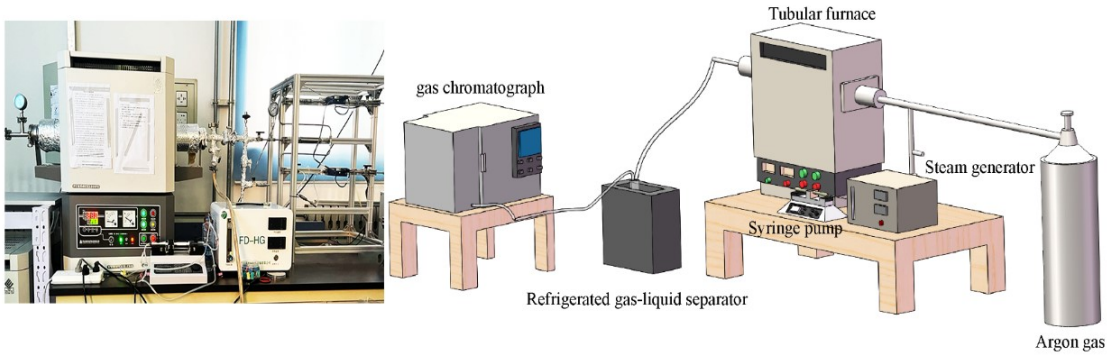

Fig. S1 Experimental setup of the redox reaction and gas detection process.

XRD result

Fig. S2 shows the XRD results of CeO_2 before and after the thermochemical H_2 production cycles. CeO_2 remains the stable lattice structure after experiments. A good fit of the synthesized materials with the PDF graph of CeO2 (PDF #81-0792) has been obtained in this part.

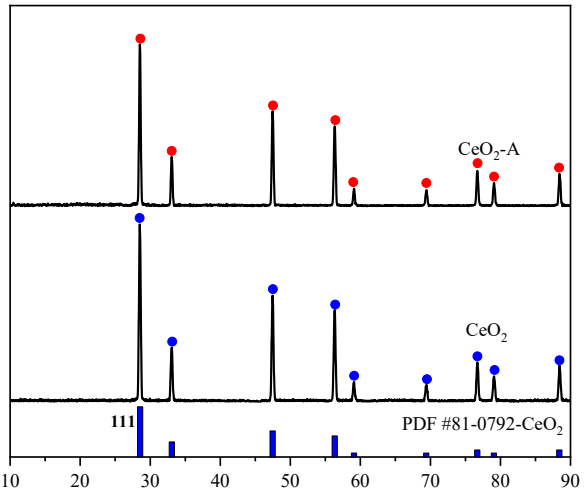

Fig. S2 XRD patterns of the ready-made Ceria (A indicates the results after experiments)

As shown in Fig. S3, the Bragg peaks of CeO_2 appear in the XRD graph of $YCr_{0.75}Zr_{0.25}O_3$-25wt% CeO_2 after experiments. The mixing of CeO_2 causes the downshift of the main peak (121) because of the large ionic radius of Ce^{4+}(0.87 Å). The calculated lattice structures and parameters are listed in Table S2.

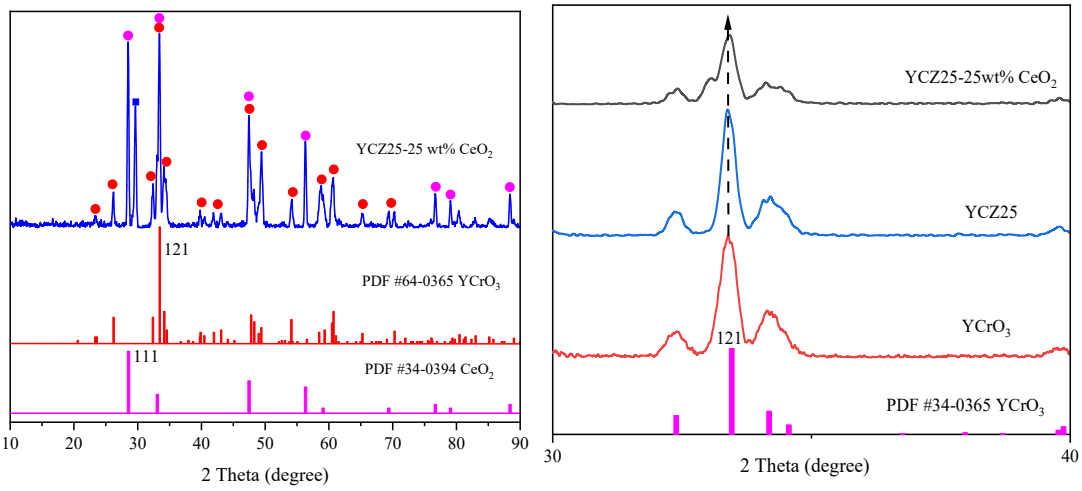

Fig. S3 XRD patterns of the mixed $YCr_{0.75}Zr_{0.25}O_3$-25wt% CeO_2 after experimental process.

Table S2. XRD calculation results of $YCr_{0.75}Zr_{0.25}O_3$-25wt% CeO_2

Samples	Lattice constants and angles	Crystalline size(nm)	d (1 2 1) (Å)
YCZ25-25wt% CeO_2	a=5.517 Å, b=7.54 Å, c=5.26 Å, $\alpha=\beta=\gamma=90°$	28.0	2.681

SEM result

Fig. S4 shows the SEM graphs of $YCr_{0.75}Zr_{0.25}O_3$-25 wt% CeO_2 after the thermochemical reactions, which shows a multi-porous structure..

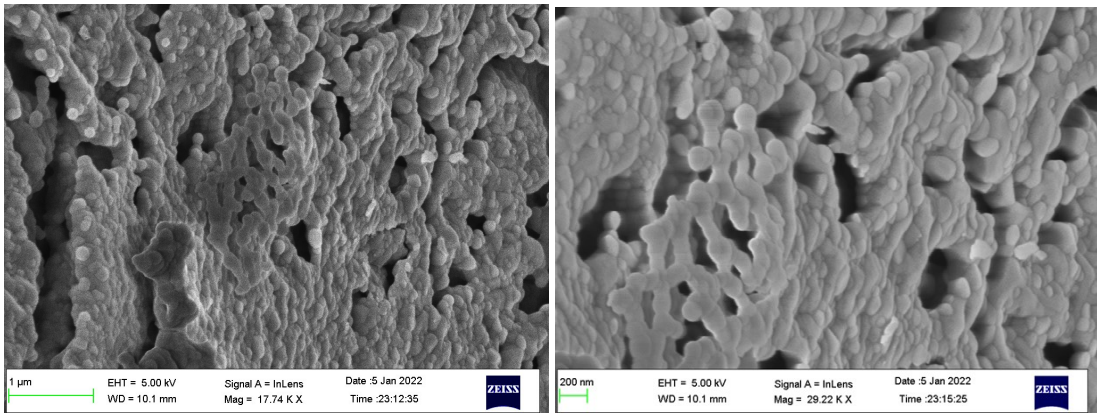

Fig. S4 SEM graphs of $YCr_{0.75}Zr_{0.25}O_3$-25 wt% CeO_2

EDX result

Fig. S5 indicates the EDX result of elemental composition of the synthesized material $YCr_{0.75}Zr_{0.25}O_3$.

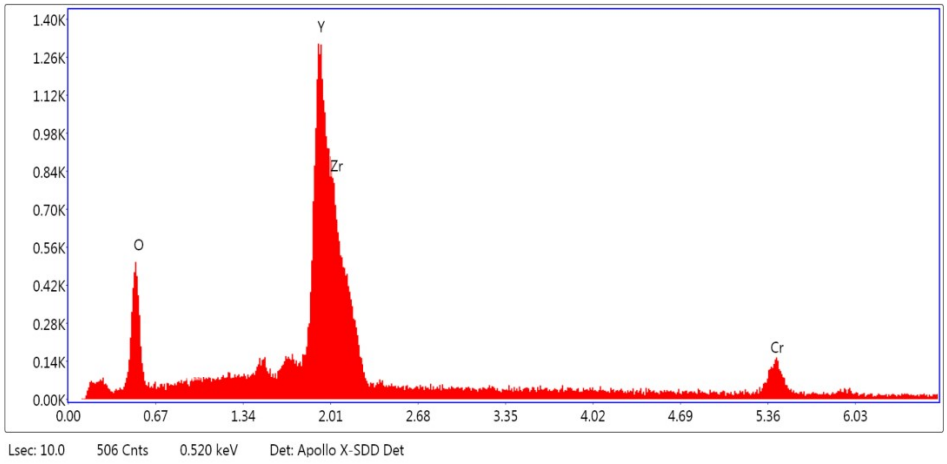

Fig. S5 EDX mapping of the Y, Cr and Zr distribution in the $YCr_{0.75}Zr_{0.25}O_{3-\delta}$ sample

Zr doping ratio

Fig. S6 shows the H_2 production capacity under different Zr doping ratios (10, 25, 40 mol%).

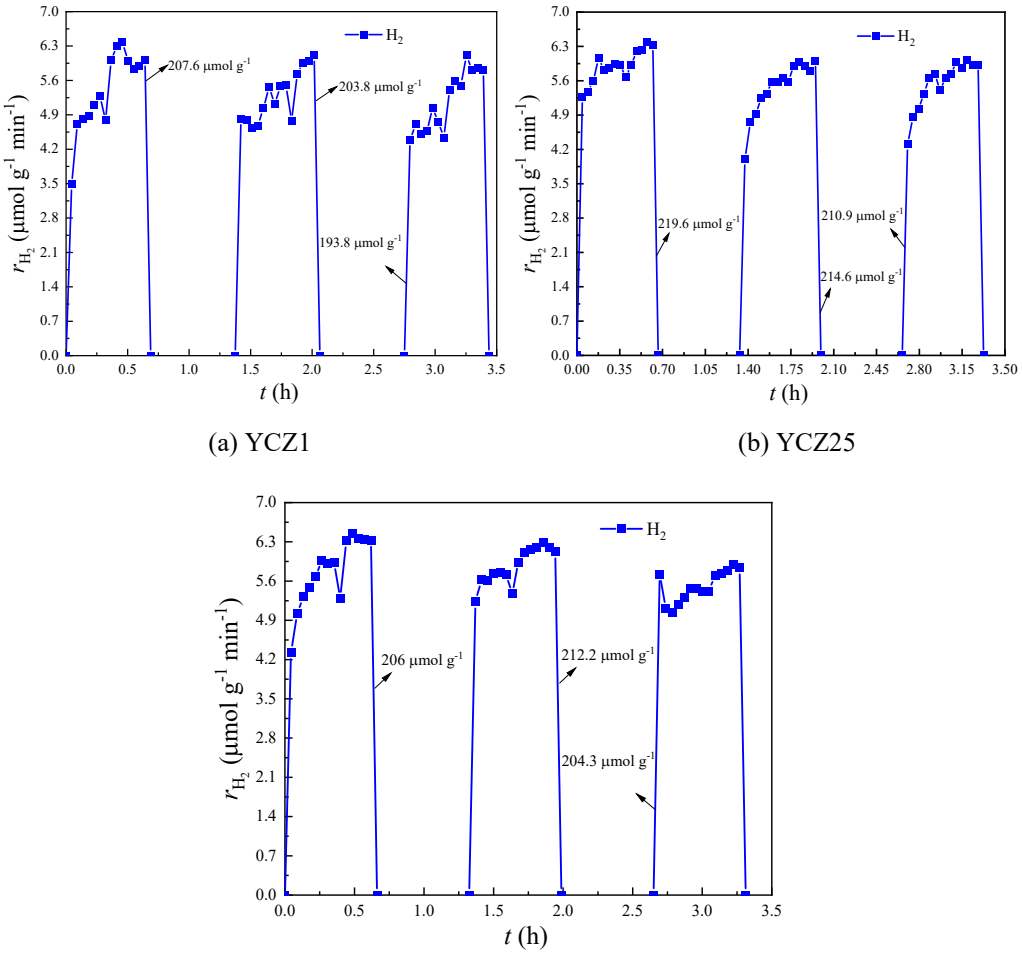

(a) YCZ1 (b) YCZ25

(c) YCZ4

Fig. S6 The H_2 rate under different Zr doping ratios (10, 25, 40 mol%). Materials were reduced at 1400

°C (heated at 10 °C/min) and oxidized at 1300 °C (cooled at 30 °C/min) in the 40 min water-splitting process

The comparison of H_2 yield of three Zr doping ratios

To determine the optimum doping ratio of Zr, the STWS performance of three Zr doping ratios (10, 25, 40 mol%) are compared in the Fig. S7. Based on the comparison results of different Zr doping ratios, the doping of Zr at 25 mol% presents the favorable H_2 yield (Y_{H_2}=219.6 μmol g^{-1}). On the whole, H_2 yield of multiple cycles under the three Zr doping ratios show a gradual decrease trend except a slight increase of YCZ4, which may be caused by the remove of impurities contained in the parent and the release of excess oxygen have limited H_2 production ability of the first STWS cycle. By comparing H_2 yield loss of different Zr doping ratios, YCZ1 shows the most considerable decrease of H_2 production capacity and YCZ25 has the lowest rate of decline. As for the whole H_2 production performance of the three cycles, the Y_{H_2} of YCZ25 is higher than the value of YCZ1 and YCZ4. From the above analysis, the setting of Zr doping ratio at 25 mol% can achieve the favorable performance of H_2 production.

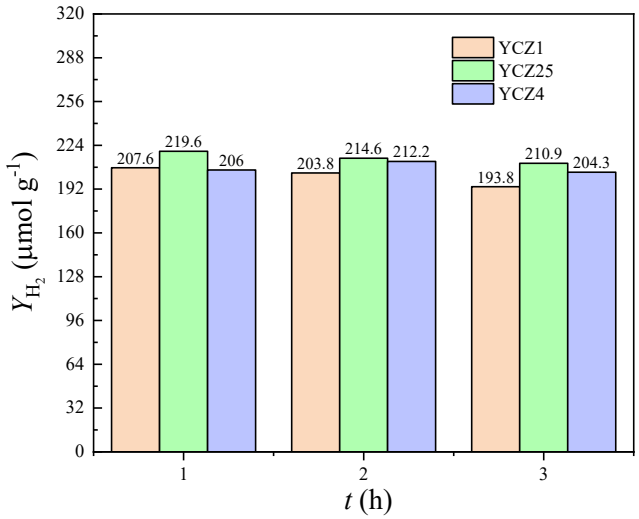

Fig. S7 The H_2 yield per mass and rate per minute of YCZ1, YCZ25 and YCZ4. Materials were reduced at 1400 °C (heated at 10 °C/min) and oxidized at 1300 °C (cooled at 30 °C/min) in the 40 min water-splitting process

Ceria mixing ratio

After the determination of Zr doping ratio, we try to mix ceria in 25 mol% Zr doped $YCrO_3$

materials to improve the water-splitting kinetic performance. Fig. S8 shows the H_2 production performance of three STWS cycles under different ceria mixing ratios. The ceria mixing ratio of 25 wt% shows a favorable H_2 production performance compared with the ceria ratio of 10 wt% and 50 wt%.

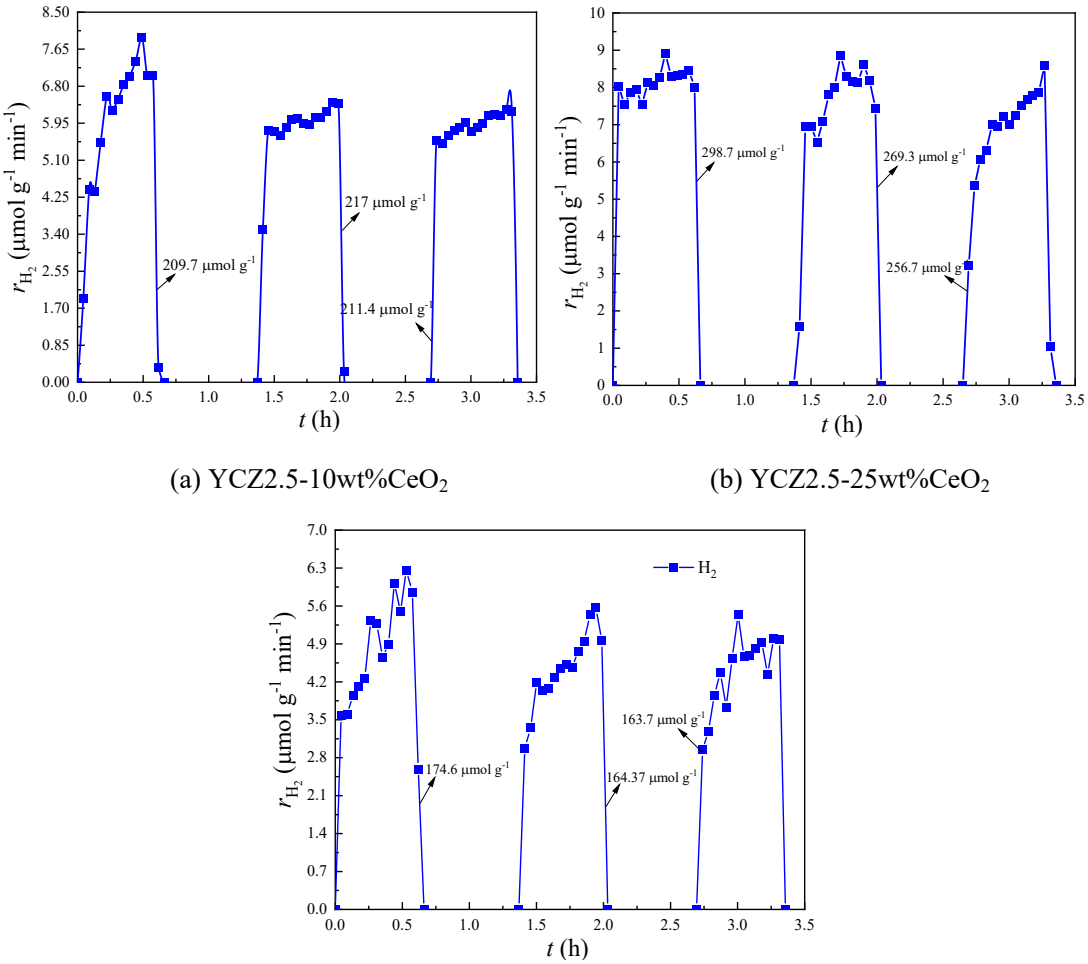

(a) YCZ2.5-10wt%CeO_2 (b) YCZ2.5-25wt%CeO_2

(c) YCZ2.5-50wt%CeO_2

Fig. S8 Hydrogen production under different ceria mixing ratios (10, 25, 50 wt% CeO_2). Materials were reduced at 1400 °C (heated at 10 °C/min) and oxidized at 1300 °C (cooled at 30 °C/min) in the 40 min water-splitting process

The comparison of H_2 yields of three ceria mixing ratios

The comparison of H_2 yield of three ceria mixing conditions (10, 25 and 50 wt%) are shown in the Fig. S9. In the multiple cycles, the H_2 yields of mixture materials indicated a slight decrease trend, the maximum variation of H_2 yields was 9.8% and the minimum change was 0.4%. In the STWS cycles, the ceria mixture ratio of 25 wt% performs the optimum performance, and the average

H_2 yield of this condition is 274.9 μmol g^{-1}. The average H_2 yields of YCZ25-10wt%CeO_2 and YCZ25-50wt%CeO_2 are 22.7% and 39.1% lower than YCZ25-25wt%CeO_2. From the above analysis, the suitable ceria mixing ratio can stimulate water splitting in the STWS process and the excess of ceria influences the H_2 yields because of the weakness of reduction capacity. On the basis of the determined Zr doping ratio, ceria mixing ratio at 25% can further lead to 27.8% increase of H_2 yield.

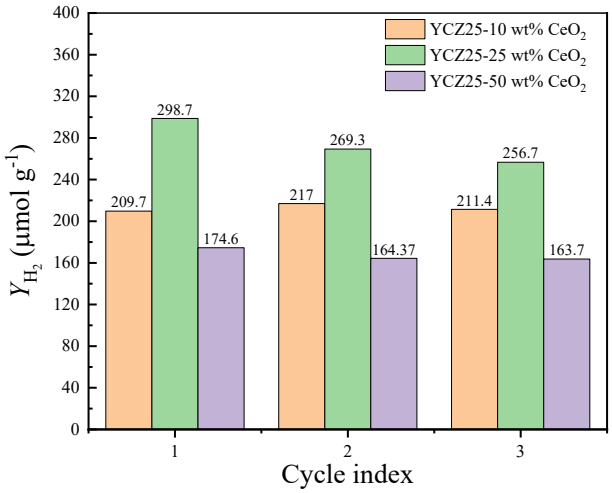

Fig. S9 The H_2 yield of YCZ25-10 wt%CeO_2, YCZ25-25wt%CeO_2 and YCZ25-50wt%CeO_2. Materials were reduced at 1400 °C (heated at 10 °C/min) and oxidized at 1300 °C (cooled at 30 °C/min) in the 40 min water-splitting process